Vecuronium bromide and its advanced intermediates: a crystallographic and spectroscopic study

Samuele Ciceri [a,*], Diego Colombo [b], Patrizia Ferraboschi [b], Paride Grisenti [c], Marco Iannone [d], Matteo Mori [a], Fiorella Meneghetti [a]

[a]*Department of Pharmaceutical Sciences, University of Milan, Via L. Mangiagalli 25, 20133 Milano, Italy*
[b]*Department of Medical Biotechnology and Translational Medicine, University of Milan, Via C. Saldini 50, 20133 Milano, Italy*
[c]*Chemical-Pharmaceutical Consulting and IP Management, Viale G. da Cermenate 58, 20141 Milano, Italy*
[d]*Department of Medicine and Surgery, Tecnomed Foundation, University of Milano-Bicocca, Monza, Italy*

Keywords: amino-androstane, vecuronium, neuromuscular blocking agent, muscle relaxant, general anesthesia, NMR, X-ray, Hirshfeld surface analysis.

*Corresponding author:
Samuele Ciceri
University of Milan - Department of Pharmaceutical Sciences
Via L. Mangiagalli 25 - 20133 Milano
Tel: ++39-02-50319306
e-mail: samuele.ciceri@unimi.it

Highlights:

- Neuromuscular blocking agents (NMBAs) induce relaxation of the skeletal muscles.
- Vecuronium bromide was synthesized in higher yield, optimizing the literature synthetic process.
- A complete analytical characterization of vecuronium bromide and its synthetic intermediates was reported to fill the literature gap.
- Using the single-crystal X-ray diffraction (SC-XRD) technique, we unambiguously described the stereochemistry of **10**, a key intermediate for the synthesis of several NMBAs.

ABSTRACT

Vecuronium bromide (Piperidinium, 1-[(2β,3α,5α,16β,17β)-3,17-bis(acetyloxy)-2-(1-piperidinyl)androstan-16-yl]-1-methyl-, bromide; Norcuron®) has been extensively used in anesthesiology practice as neuromuscular blocking agent since its launch on the market in 1982. However, a detailed crystallographic and NMR analysis of its advanced synthetic intermediates is still lacking. Hence, with the aim of filling this literature gap, vecuronium bromide was prepared starting from the commercially available 3β-hydroxy-5α-androstan-17-one (epiandrosterone), implementing some modifications to a traditional synthetic procedure. A careful NMR study allowed the complete assignment of the ^{1}H, ^{13}C, and ^{15}N NMR signals of vecuronium bromide and its synthetic intermediates. The structural and stereochemical characterization of 2β,16β-bispiperidino-5α-androstane-3α,17β-diol, the first advanced synthetic intermediate carrying all the stereocenters in the final configuration, was described by means of single-crystal X-ray diffraction and Hirshfeld surface analysis, allowing a detailed conformational investigation.

1. INTRODUCTION

Neuromuscular blocking agents (NMBAs) are widely used in general anesthesia to induce relaxation of the skeletal muscles, facilitating surgery and endotracheal intubation. These agents are structurally related to the endogenous neurotransmitter acetylcholine (**1**, Figure 1) and classified as either depolarizing or non-depolarizing agents, based on their mechanism of action [1, 2].

Depolarizing agents depolarize the plasma membrane of the skeletal muscle, acting as agonists on the acetylcholine receptors located on the neuromuscular junction, while non-depolarizing agents are competitive antagonists of acetylcholine. The incorporation of an acetylcholine-like fragment in an androstane skeleton led to the development of a series of highly active and selective non-depolarizing NMBAs [3]: pancuronium bromide (**2**), pipecuronium bromide (**3**), vecuronium bromide (**4**), rocuronium bromide (**5**), rapacuronium bromide (**6**), and SZ-1677 (**7**) (Figure 1).

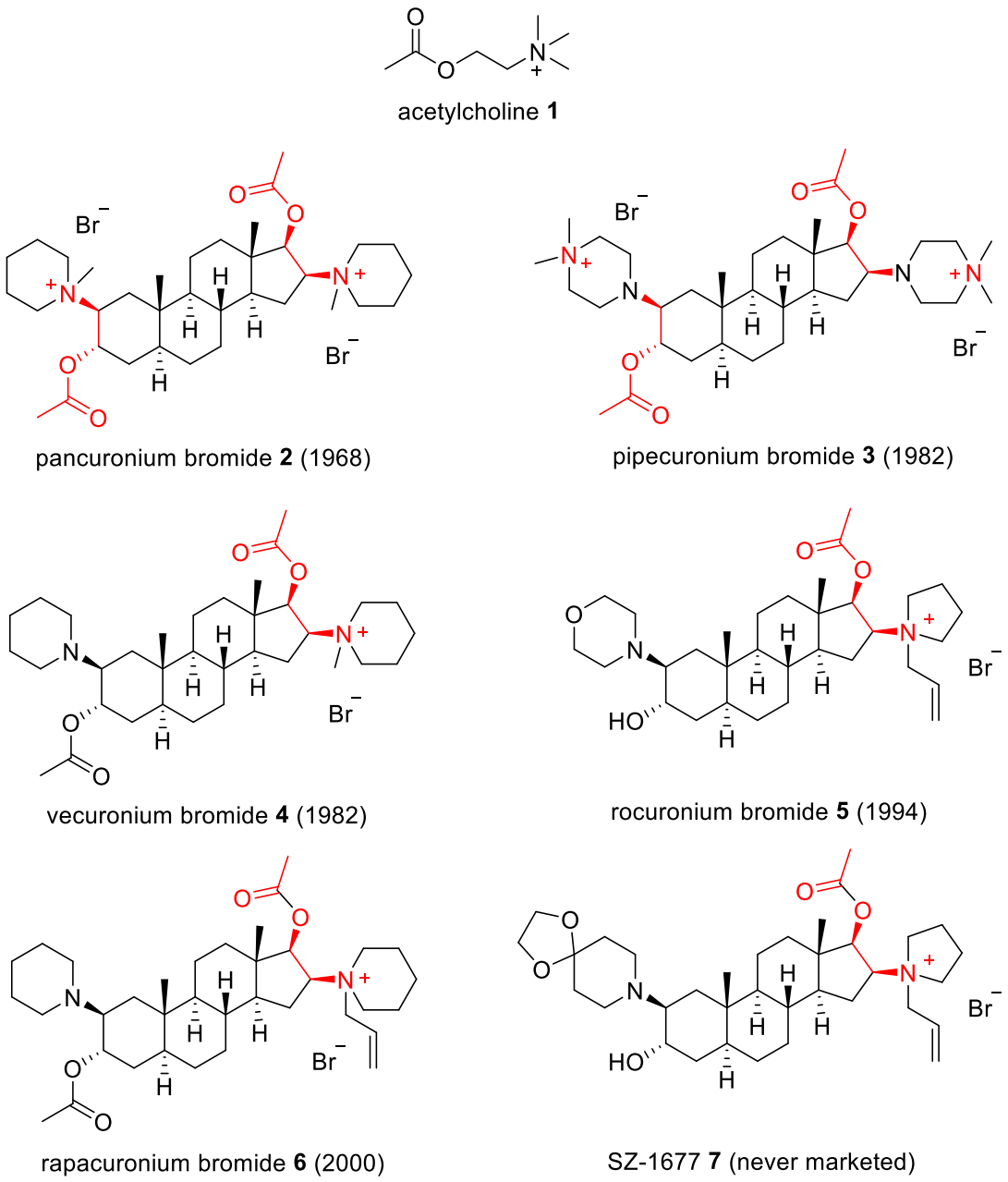

Figure 1. Chemical structures of the endogenous neurotransmitter **1** and of NMBAs **2-7**. The year of their commercialization is reported in brackets. The acetylcholine-like fragments are indicated in red.

The members of this series differ from each other in their potency, onset time, duration of action, and side effects [4] (Table 1).

Table 1. Pharmacokinetics and cardiovascular side effects of NMBAs **2-6**. ED_{95} is the 95% effective dose. Data may vary depending on patient characteristics. Source: ref. [4].

NMBA	ED_{95} (μmol/Kg)	Dose (mg/Kg; 2 x ED_{95})	Onset (min)	Duration (min)	Recovery index (min)	Cardiovascular effects
2	0.1	0.15	3÷5	90÷120	30÷45	✓
3	0.07	0.1	3÷5	90÷120	30÷45	×
4	0.07	0.1	3÷4	35÷45	10÷15	×
5	0.6	0.6	1.5÷3	30÷40	10÷15	✓

6	1.5	2.0	1÷1.5	15÷25	5÷7	✓

Vecuronium bromide (**4**) was described for the first time in 1965 by Hewett and Savage [5] and has been used in anesthesiology since its launch in 1982 under the brand name Norcuron®. To date, it is the most specific NMBA used in clinical practice, characterized by a fast onset time and an intermediate duration of action (Table 1). Compared to other NMBAs, **4** has fewer side effects, showing a low propensity to release histamine and to affect the cardiovascular system [6]; moreover, in case of necessity, its neuroblocking activity can be reversed by sugammadex [7]. The presence of **4** in the "World Health Organization's List of Essential Medicines" [8] underlines the importance of this drug for the healthcare system. Furthermore, the use of this agent is not restricted to humans but can be extended to animals, such as dogs, cats, horses, and sheep [6].

Although the synthesis of **4** from 2α,3α:16α,17α-diepoxy-17β-acetoxy-5α-androstane (**8**) has been known for decades [5, 9] (Scheme 1), only a few spectroscopic and crystallographic studies are reported in the literature.

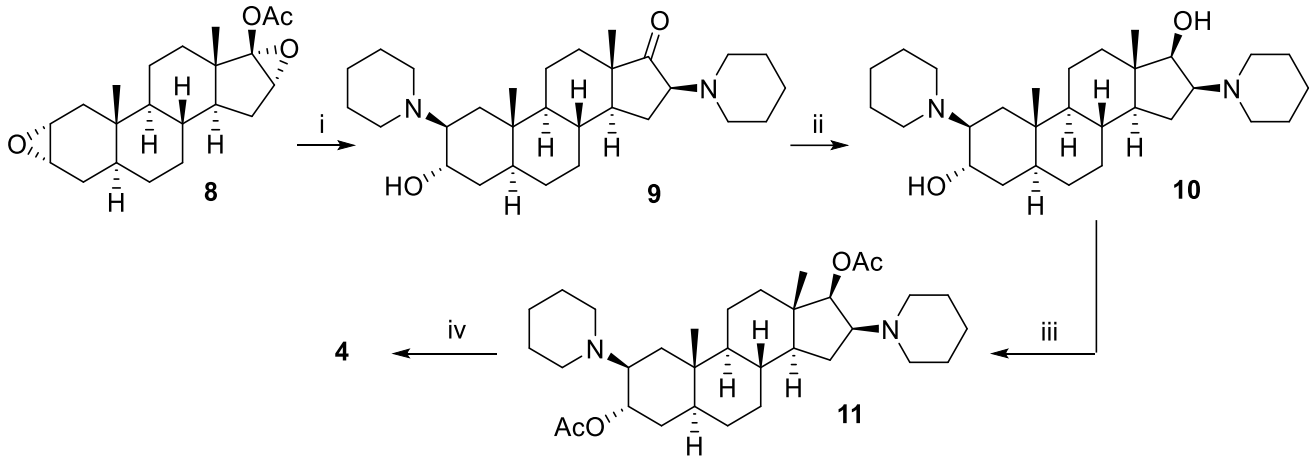

Scheme 1. Literature reported synthesis of **4**: ref. [5, 9]. (i) Piperidine, H_2O, reflux, 3-5 days, 66%; (ii) $NaBH_4$, $MeOH/CH_2Cl_2$, 18 °C, 18 h, 96%; (iii) Ac_2O, 90 °C, 1 h, 39%; (iv) CH_3Br, Et_2O, yields not declared.

The molecular structure of **4** was determined in 1991 [10] by SC-XRD analysis and the complete assignment of its ^{1}H and ^{13}C NMR resonances (400 and 100 MHz, respectively) was reported in 1998 [11].

The assignment of the ^{1}H and ^{13}C NMR signals of intermediate **10** was reported in a 2008 Chinese paper [12] together with the interpretation of the ^{13}C spectra of intermediates **8**, **9**, and **11**. These incomplete NMR and crystallographic analyses prompted us to gather new and more conclusive data for **8**-**11**. In a continuing effort to fully characterize molecules that exert important therapeutic properties [13-15], a complete NMR (^{1}H, ^{13}C, ^{15}N) characterization of compounds **8**-**11**, and **4** was carried out. Furthermore, a detailed crystallographic investigation performed on the valuable

synthetic intermediate **10**, suitable for the synthesis of **4** as well as of **2** and **6**, allowed the complete stereochemical assignment of its stereocenters and the deeper description of its geometrical features.

2. EXPERIMENTAL

2.1 General

All reagents and solvents were purchased from Sigma-Aldrich (Merck Life Science S.r.l., Milano, Italy). 3β-Hydroxy-5α-androstan-17-one (epiandrosterone) was purchased from Syntex (Cuernavaca, Morelos, Mexico). TLC analyses were performed on silica gel 60 F_{254} plates, precoated with a fluorescent indicator (Merck Life Science S.r.l., Milano, Italy); spots were detected by a 0.3% *w*/*v* ninhydrin solution in *n*-butanol/acetic acid (100:3) and heating at 110 °C, or by a 5% phosphomolybdic acid solution in ethanol and heating at 110 °C.

2.2 Chemistry

*2.2.1 2α,3α:16α,17α-Diepoxy-17β-acetoxy-5α-androstane (**8**)*

To a solution of epiandrosterone (100 g; 344.3 mmol) in anhydrous pyridine (250 mL), *p*-toluenesulfonyl chloride (100 g; 524.5 mmol) was added. The solution was stirred at room temperature for 20 hours and then poured into an ice/water mixture (1 L). The obtained solid was recovered by suction, washed with water (3 x 200 mL), and dried (40 °C; 2 mmHg; 8 h) affording the tosyl derivative of epiandrosterone (140.9 g; 316.8 mmol; 92%). The chemical and physical properties were in agreement with literature data [16].

The tosyl derivative of epiandrosterone (71.0 g; 159.6 mmol) was added to a mixture of glacial acetic acid (660 mL), acetic anhydride (66 mL) and sodium acetate (73.5 g). The reaction mixture was refluxed for 2 hours, poured into water (2.5 L), and extracted with chloroform (3 x 500 mL). The combined organic layers were washed with a saturated aqueous solution of sodium carbonate (500 mL), with water (500 mL), and dried over sodium sulfate. After evaporation of the solvent under reduced pressure, crude 5α-androst-2-ene-17-one **13** (47.9 g) was obtained. The crude product was suspended in a mixture of methanol (1.5 L), water (220 mL), and potassium hydroxide (29.0 g) and refluxed for 30 minutes. The reaction mixture was stirred at room temperature overnight. The obtained white precipitate was recovered by suction and dried (40 °C; 2 mmHg; 8 h) affording pure **13** (21.3 g; 78.2 mmol; 49%). The chemical and physical properties were in agreement with literature data [16].

To a solution of **13** (19.5 g; 71.6 mmol) in isopropenyl acetate (195 mL), 95-97% sulfuric acid (2.0 mL) was added. The reaction mixture was stirred at room temperature for 6 hours and poured in a saturated aqueous solution of sodium hydrogen carbonate (1 L). The precipitate was recovered by suction, washed with water (3 x 200 mL) and dried (40 °C; 2 mmHg; 8 h) affording 17β-acetoxy-5α-

androsta-2,16-diene (15.5 g; 49.3 mmol; 69%). The chemical and physical properties were in agreement with literature data [17].

To a solution of 17β-acetoxy-5α-androsta-2,16-diene (13.5 g; 42.9 mmol) in toluene (75 mL), a solution of 3-chloroperbenzoic acid (24.3 g; 70-75% in water; 102.1 mmol) in toluene (150 mL) was added dropwise (1 hour) under stirring at 0 °C. The reaction mixture was stirred at room temperature for 5 hours and washed with an ice cooled 1 M solution of sodium hydroxide (200 mL) and then with water (200 mL). The organic layer was dried over sodium sulfate and filtered. The evaporation of the solvent under reduced pressure afforded crude 2α,3α:16α,17α-diepoxy-17β-acetoxy-5α-androstane **8**. Crystallization from diethyl ether afforded pure **8** (11.9 g; 34.3 mmol; 80%). The chemical and physical properties were in agreement with literature data [17].R_f = 0.83 (*n*-hexane/EtOAc 6:4).

2.2.2 2β,16β-Bispiperidino-5α-androstan-3α-ol-17-one (**9**).

Compound **8** (10.0 g; 28.9 mmol) was suspended in freshly distilled piperidine (48 mL; 485.9 mmol) and water (16 mL). The addition was exothermic and led to the spontaneous solubilization of compound **8**. The reaction mixture was refluxed for 3 days. The reaction progress was monitored by TLC analysis. The reaction mixture was concentrated at reduced pressure (60 °C; 30 mmHg), water (50 mL) was added, and, after 1 hour of vigorous stirring, the obtained solid was recovered by suction, washed with water (3 x 20 mL) and suspended in a 2 M aqueous solution of hydrochloric acid (50 mL). After 30 minutes under stirring at room temperature, the mixture was filtered. The filtrate was cooled to 5 °C and a 10% aqueous solution of sodium hydroxide (about 30 mL) was added until a pH value of 9.5-10.0 was reached. The aqueous phase was extracted with dichloromethane (4 x 50 mL). The organic phases were collected and dried over sodium sulfate, filtered and concentrated under reduced pressure to afford a white foamy solid (14.9 g). This solid was dissolved in anhydrous acetone (50 mL). After few minutes under stirring at 5 °C, the formation of a white solid was observed. The stirring was maintained for 1 hour at 5 °C, then the solid was recovered by suction, washed with cold acetone (2 x 10 mL) and dried (2 mmHg, 25 °C, 16 h) affording compound **9** (5.7 g; 12.4 mmol; 43% yield). The chemical and physical properties were in agreement with literature data [9].

R_f = 0.62 ($CHCl_3$/MeOH/H_2O 12.5:4.0:0.5).

2.2.3 2β,16β-Bispiperidino-5α-androstan-3α,17β-diol (**10**)

Compound **9** (5.0 g; 10.9 mmol) was dissolved in a mixture of methanol (19.5 mL) and dichloromethane (6.5 mL). Under stirring, sodium borohydride (625 mg; 16.5 mmol) was slowly added maintaining the reaction mixture at about 18 °C. The reaction mixture was stirred at room

temperature for 4 h. Then, the solvent was removed under reduced pressure (30 °C; 30 mmHg) and water (50 mL) was added. The mixture was stirred at room temperature for 1 hour. The white solid was recovered by suction, washed with water (3 x 20 mL) and dried (2 mmHg, 25 °C, 16 h) affording compound **10** (4.8 g; 10.5 mmol; 96%). The chemical and physical properties were in agreement with literature data [9].

R_f = 0.37 ($CHCl_3$/MeOH/H_2O 12.5:4.0:0.5).

2.2.4 2β,16β-Bispiperidino-3α,17β-diacetoxy-5α-androstane (**11**)

$ZnCl_2$ (350 mg; 2.6 mmol) was added to a solution of compound **10** (4.0 g; 8.7 mmol) in acetic anhydride (14 mL; 148.1 mmol) and acetic acid (3.5 mL; 61.2 mmol). The reaction was stirred at room temperature under a nitrogen atmosphere for 3 hours. The reaction was monitored by TLC ($CHCl_3$/MeOH/H_2O 12.5:4.0:0.5). The mixture was poured into water (180 mL) and, under stirring at 0÷5 °C, a 6% aqueous solution of ammonium hydroxide (about 128 mL) was added to reach pH 9.0-9.5. The mixture was extracted with *tert*-butyl-methyl ether (3 x 100 mL). The collected organic phases were washed with water (3 x 100 mL) and dried over sodium sulfate; after filtration, the solvent was removed under reduced pressure to afford **11** as a white solid (4.3 g; 7.9 mmol; 91%), which was used in the next step without further purification. For analytical purposes, a sample (0.5 g) was purified by crystallization from acetonitrile.

R_f = 0.71 ($CHCl_3$/MeOH/H_2O 12.5:4.0:0.5).

2.2.5 Piperidinium, 1-[(2β,3α,5α,16β,17β)-3,17-bis(acetyloxy)-2-(1-piperidinyl)androstan-16-yl]-1-methyl-, bromide (vecuronium bromide) (**4**)

To a solution of **11** (2.0 g; 3.7 mmol) in ethyl ether (30 mL), methyl trifluoromethanesulfonate (0.42 mL; 3.7 mmol) was added under a nitrogen atmosphere. Stirring the reaction mixture for 20 minutes at 25 °C resulted in the formation of a white precipitate. The solid was recovered by suction and washed with ethyl ether (2 x 8 mL). Then, it was suspended in ethyl ether (20 mL), stirred at room temperature for about 30 minutes and recovered by suction. After drying (2 mmHg; 45 °C), vecuronium trifluoromethanesulfonate was obtained as a white solid (2.4 g; 3.4 mmol; 92%). The chemical and physical properties were in agreement with literature data [18].

To a solution of the previously obtained vecuronium trifluoromethanesulfonate (2.0 g; 2.8 mmol) in acetone (20 mL), lithium bromide (1.0 mg; 11.5 mmol) was added. The reaction mixture was stirred for 20 minutes at 25 °C, until the formation of a white precipitate of lithium methanesulfonate. Ethyl ether (20 mL) was added, and the reaction mixture was stirred for additional 10 minutes. The solid was recovered by suction and washed with a 1:1 mixture of ethyl ether/acetone (2 x 20 mL). After

drying (2 mmHg; 60 °C), crude **4** was obtained as a slightly pink-colored solid (2.3 g). Crude **4** was suspended in a 1:1 mixture of CH_2Cl_2/H_2O (30 mL) and stirred for 30 minutes at room temperature. Then the phases were separated and the aqueous layer was extracted with CH_2Cl_2 (2 x 15 mL). The collected organic phases were dried over sodium sulfate, filtered, and evaporated under reduced pressure (30 mmHg; 30 °C) affording **4** as a slightly pink-colored solid (1.5 g; 2.4 mmol; 86% yield). The chemical and physical properties were in agreement with literature data [18].

2.3 NMR spectroscopy

NMR spectra were recorded on a Bruker AVANCE 500 spectrometer (Bruker, Billerica, MA, USA) equipped with a 5 mm broadband inverse (BBI) detection probe with field z-gradient operating at 500.13, 125.76, and 50.69 MHz for ^{1}H, ^{13}C, and ^{15}N, respectively. The spectra were recorded at 325 K for **8**-**11**, and **4** in pyridine-d_5 (isotopic enrichment 99.9 atom % D). The central peak of pyridine-d_5 signals (7.0 ppm, higher field signal, for ^{1}H, 123.4 ppm, higher field signal, for ^{13}C spectra [19], and 317 ppm for ^{15}N spectra [20], respectively) was used as an internal reference standard. Data were collected and processed by XWIN-NMR software (version 3.5, Bruker, Billerica, MA, USA) running on a PC with Microsoft Windows 7. The samples (20 mg) were dissolved in the appropriate solvent (0.6 mL) in a 5 mm NMR tube. The acquisition parameters for 1D were as follows: ^{1}H spectral width of 5000 Hz and 32 K data points providing a digital resolution of ca. 0.153 Hz per point, relaxation delay 10 s; ^{13}C spectral width of 29499 Hz, and 32 K data points providing a digital resolution of ca. 0.900 Hz per point, relaxation delay 2 s. The experimental error in the measured ^{1}H-^{1}H coupling constants was ±0.5 Hz. The splitting pattern abbreviations are as follows: s, singlet; d, doublet; t, triplet; q, quartet; m, multiplet; and br, broad signal. Except for NOESY, for two-dimensional experiments standard Bruker microprograms using gradient selection (gs) were applied. Gs-COSY-45 and phase-sensitive NOESY experiments were acquired with 512 t_1 increments, 2048 t_2 points, and a spectral width of 6.0 ppm. The NOESY experiments were performed with a mixing time of 0.800 s on samples degassed under a flush of argon in a screwcap sample tube. There were not significant differences in the results obtained at different mixing times (0.5–1.5 s). The acquisition data for gs-HSQC and gs-HMBC experiments were acquired with 512 t_1 increments, 2048 t_2 points, and a spectral width of 6.0 ppm for ^{1}H and 200 ppm for ^{13}C. Delay values were optimized to 140 Hz for $^{1}J_{C,H}$ and 8.0 Hz for $^{n}J_{C,H}$.

The gs-^{1}H-^{15}N HMBC experiments, were performed setting an acquisition time of 0.5 s, a relaxation delay of 10 s, a $^{1}J_{N,H}$ value of 90.0 Hz, and a $^{n}J_{N,H}$ value of 5.0 Hz. This last parameter was set after several attempts between 1 and 10 Hz. The total experimental time for ^{1}H-^{15}N gs-HMBC analyses was 12 hours.

In the “Results and Discussion” section, steroid carbons are labelled in the conventional fashion as reported in Figure 2.

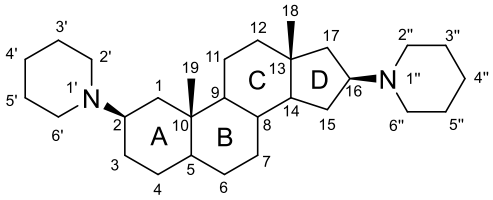

Figure 2. Conventional labelling of steroid carbons and rings.

2.4 Single-crystal X-ray and Hirshfeld surface analysis

Crystals of **10** were obtained at room temperature as colorless prisms from a 3:1 $CHCl_3$/EtOH solution. X-ray intensity data were collected at 293 K with a Rigaku XtaLAB Synergy-S diffractometer, equipped with a microfocus Mo-Kα source and a HyPix-6000HE detector, and operated at 50 kV and 1 mA. Data collection was performed with omega scans with a step size of 1° and an exposure time of 30 s/frame. A total number of 54491 Bragg reflections (with a high degree of redundancy) were collected, giving a metrically monoclinic unit. The analysis of the systematic absences suggested the space group $P2_1$. Intensity data were integrated and corrected for Lorentz-polarization effects, using the computer program Rigaku CrysAlisPRO 1.171.41.105a (CrysAlisPro Software System, Rigaku Oxford Diffraction/Agilent Technologies UK Ltd, Yarnton, UK); an analytical absorption correction was applied by Gaussian integration based on the physical description of the crystal. The structure was solved by direct methods using SIR2014 [21] and completed by iterative cycles of full-matrix least squares refinement on F_o^2 and ΔF synthesis using SHELXL-2018/3 [22] within the WinGX suite (WinGX v.2014.1) [23]. Hydrogen atoms were introduced at calculated positions in their described geometries and allowed to ride on the attached atom with fixed isotropic thermal parameters (1.2 U_{eq} and 1.5 U_{eq} of the parent atom for methylene and methyl/hydroxyl groups, respectively). The structure was analyzed with PARST [24], and the graphical representations were rendered with Mercury 2020.2.0 [25]. Hirshfeld surface (HS) analysis was performed with CrystalExplorer 17 [26].

Crystal data for 10. Formula: $C_{29}H_{50}N_2O_4$; MW = 458.72 g/mol; Bravais lattice: monoclinic; space group: $P2_1$; cell dimensions: a = 6.1944(3) Å, b = 11.3618(4) Å, c = 19.2649(9) Å, β = 97.044(4)°; V = 1345.62(10) $Å^3$; Z = 2; D_{calc} = 1.132 Mg/m^3; $2\theta_{min}$ = 2.085°; $2\theta_{max}$ = 37.552°; limiting indices = $-10 \le h \le 10$, $-19 \le k \le 19$, $-31 \le l \le 32$; crystal size: 0.88 × 0.12 × 0.11 mm; T = 293(2) K; F(000) = 508; R_{int} = 0.1049; R = 0.0671 for 5529 reflections with $F_o > 4\text{sig}(F_o)$ (R = 0.1861 for all 12914 unique/54491 collected reflections), wR2 = 0.1422 for reflections with $F_o > 4\text{sig}(F_o)$ (wR2 = 0.1773 for all unique reflections); GOOF = 0.989; Residual positive and negative electron densities in the final map: 0.162 and −0.196 $Å^{-3}$.

Hirshfeld analysis data for 10. Volume: 664.72 Å^3; area: 498.71 Å^2; globularity (*G*): 0.739; asphericity (*Ω*): 0.354.

Full experimental data can be obtained free of charge *via* www.ccdc.cam.ac.uk/conts/retrieving.html (or from the Cambridge Crystallographic Data Centre, 12, Union Road, Cambridge CB21EZ, UK; fax: ++44 1223 336 033; or deposit@ccdc.cam.ac.uk). CCDC entry 2081434 contains supplementary crystallographic data for this paper.

3. RESULTS AND DISCUSSION

3.1 Chemistry

Ten stereogenic centers are present in the molecule of **4**, namely at C-2, C-3, C-5, C-8, C-9, C-10, C-13, C-14, C-16, and C-17, with the configuration reported in Figure 1. The stereochemistry of C-5, C-8, C-9, C-10, C-13, and C-14 is fixed, considering that they derive from the advanced intermediate **8** and remain unaffected by the synthetic process.

The two piperidino groups are usually introduced at C-2 and C-16 by heating **8** under reflux in a mixture of piperidine and water [9]. The desired 2β,16β-bispiperidino-5α-androstan-3α-ol-17-one (**9**) is then isolated by crystallization from acetone. The reduction of the carbonyl function at the 17-position with sodium borohydride proceeds in almost quantitative yields to give 2β,16β-bispiperidino-5α-androstan-3α,17β-diol (**10**), the first advanced synthetic intermediate endowed with all the stereocenters present in the final APIs **2**, **4**, and **6** (Scheme 1). The high stereoselectivity observed in this synthetic step can be explained by comparing the hindrance on the α and β faces of the 16β-bispiperidino 17-ketone **9** and its 16α-epimer **14**, which are in equilibrium under weakly alkaline conditions [9] (Scheme 2).

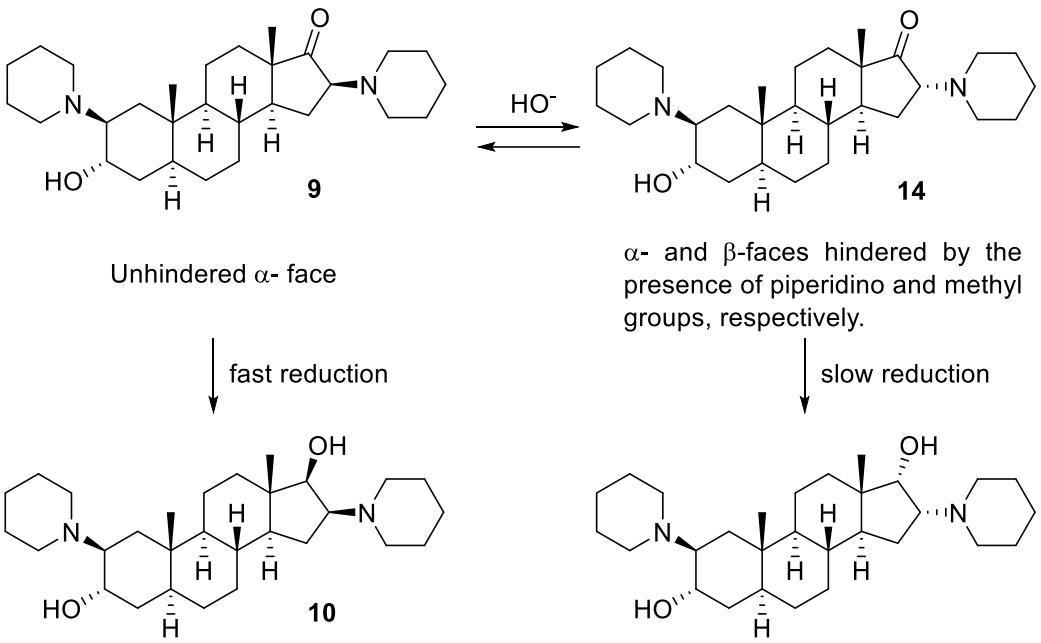

Scheme 2. Explanation of the highly stereoselective reduction of **9** to **10**.

Finally, **4** is obtained starting from intermediate **10** by acetylation of the two hydroxyl groups and quaternarization of the piperidine at the 16-position using methyl bromide (Scheme 1).

We prepared **4** and its synthetic intermediates, suitable for the crystallographic and spectroscopic studies, starting from **12** (Scheme 3). According to a validated procedure reported in the literature [16, 17], **8** was obtained starting from **12** in 25% overall yield. Following the procedure described by Buckett *et al.* [9], we prepared intermediate **10** in 41% yield, starting from **8**. Due to the low yield (39%) reported in the 1965 patent [5] for the obtainment of **11** from **10** using acetic anhydride at 90 °C, we decided to carry out the acetylation step by applying the experimental procedure described by Tuba [17] for the acetylation of 2β,16β-(4'-methyl-1'-piperazino)-5α-androstan-3α,17β-diol, a close analogue of **10**. By adapting this experimental procedure, we synthetized **11** from **10** in 91% yield.

Compound **4** was finally obtained from **11** avoiding the hazardous methyl bromide and using methyl trifluoromethanesulfonate as alkylating agent, followed by anion exchange with lithium bromide, as reported in a 2006 patent [18]. According to this procedure, the title compound **4** was obtained in 72% yield from **10**, and 30% overall yield from **8**.

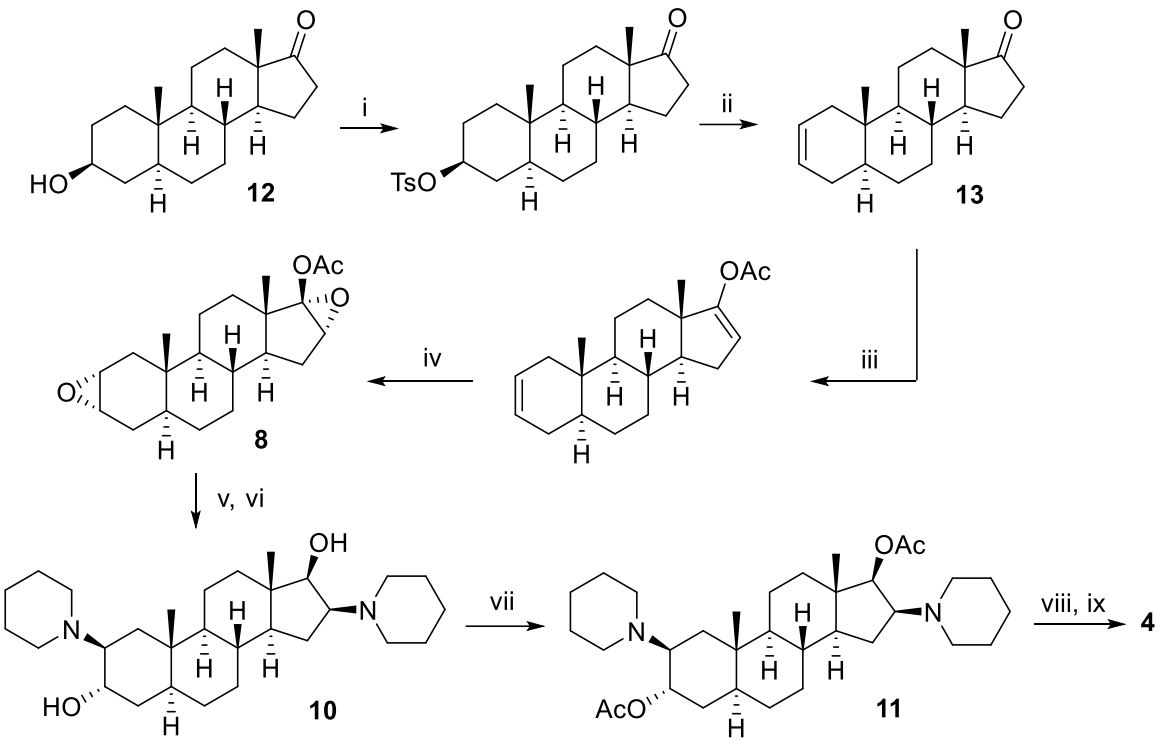

Scheme 3. Synthesis of **4** from **12**. (i) *p*-TsCl, pyridine, rt, 20 h, 92%; (ii) AcONa, Ac_2O, AcOH, reflux, 2 h, 49%; (iii) $CH_3COOC(CH_3)=CH_2$, conc. H_2SO_4, rt, 6 h, 69%; (iv) *m*-CPBA, toluene, rt, 5h, 80%; (v) Piperidine, H_2O, reflux, 3 days, 43%; (vi) $NaBH_4$, MeOH/CH_2Cl_2, rt, 4 h, 96%; (vii) Ac_2O, AcOH, $ZnCl_2$, rt, 3 h, 91%; (viii) $CF_3SO_2OCH_3$, Et_2O, rt, 20 min, 92%; (ix) LiBr, acetone, rt, 20 min, 86%.

3.2 NMR spectroscopy

A detailed NMR study was carried out on vecuronium bromide (**4**), on its precursor **8**, and on intermediates **9**-**11** (Scheme 1). NMR spectra of all the analyzed compounds were initially recorded in deuterated chloroform at 325 K, following the literature data reported for **4** [11]. However, pyridine-d_5 was finally selected as solvent because it allowed for a better resolution of the proton resonances and sharper carbon peaks for all the studied compounds. Unambiguous assignments of all ^1H, ^{13}C, and ^{15}N signals of the tested compounds (Tables 1, 2, and 3) were established by combining the information gathered from 1D NMR spectra and 2D homocorrelated (COSY and NOESY) and heterocorrelated (^1H-^{13}C HSQC, ^1H-^{13}C HMBC, and ^1H-^{15}N HMBC) NMR spectra.

Most of the proton assignments were accomplished using general knowledge of chemical shift dispersion, with the aid of the proton-proton coupling pattern (^1H NMR spectra), gs-COSY, and NOESY experiments. In ambiguous cases, gs-HSQC and gs-HMBC spectra were used as a definitive and unequivocal tool to make specific assignments.

Table 1

^1H NMR chemical shifts (ppm)[a] and coupling constants (Hz)[b] of compounds **8**-**11**, and **4**.

^1H	**8**	**9**	**10**	**11**	**4**
1α	1.17 (d, *J*=14.8 Hz)	1.36 (nd)	1.38 (nd)	1.12 (nd)	1.06 (nd)
1β	1.55 (nd)	1.54 (nd)	1.55 (nd)	1.74 (dd, *J*= 14.5 and 3.9 Hz)	1.68 (nd)

2α	2.89 (2β, m)	2.41 (nd)	2.44 (nd)	2.26 (q, *J*= 4.2 Hz)	2.23 (q, *J*= 4.5 Hz)
3β	2.85 (3β, m)	4.08 (q, *J*=5.02 Hz)	4.06 (m)	5.32 (q, *J*= 4.1 Hz)	5.29 (q, *J*= 4.0 Hz)
4α	1.61 (dd, *J*= 14.9 and 4.1 Hz)	1.46 (dt, *J*= 12.5 and 4.5 Hz)	1.46 (nd)	1.31 (nd)	1.27 (nd)
4β	1.23 (nd)	1.74 (nd)	1.75 (td, *J*= 12.7 and 5.5 Hz)	1.69 (nd)	1.63 (nd)
5α	1.11 (nd)	1.67 (tt, *J*= 12.1 and 4.2 Hz)	1.65 (tt, *J* = 12.1 and 4.3 Hz)	1.47 (nd)	1.41 (nd)
6α	0.87 (qd, *J*= 13.0 and 3.9 Hz)	1.17 (nd)	1.14 (nd)	1.10 (nd)	1.03 (nd)
6β	1.00 (nd)	1.17 (nd)	1.14 (nd)	1.10 (nd)	1.03 (nd)
7α	0.48 (ddd, *J*= 26.0, 12.8, and 4.2 Hz)	0.77 (qd, *J*=12.5 and 5.0 Hz)	0.74 (qd, *J*= 12.4 and 4.9 Hz)	0.72 (nd)	0.76 (qd, *J*= 12.3 and 5.5 Hz)
7β	1.23 (nd)	1.55 (m)	1.51 (m)	1.48 (nd)	1.45 (nd)
8β	0.96 (nd)	1.26 (m)	1.24 (nd)	1.24 (nd)	1.24 (nd)
9α	0.36 (ddd, *J*= 12.5, 9.5, and 4.6 Hz)	0.58 (ddd, *J*=12.3, 10.2, and 3.9 Hz)	0.56 (m)	0.52 (td, *J*= 12.1, 11.5 and 4.1 Hz)	0.49 (ddd, *J*= 12.2, 10.4 and 4.1 Hz)
11α	1.26 (nd)	1.41 (nd)	1.37 (nd)	1.35 (nd)	1.32 (nd)
11β	1.08 (nd)	1.13 (nd)	1.15 (nd)	1.09 (nd)	1.04 (nd)
12α	1.53 (nd)	1.11 (nd)	0.99 (td, *J*= 12.8 and 3.8 Hz)	1.04 (td, *J*= 12.5 and 3.5 Hz)	1.24 (nd)
12β	1.58 (nd)	1.72 (nd)	1.82 (dt, *J*= 12.3 and 3.4 Hz)	1.66 (m)	1.69 (nd)
14α	0.99 (nd)	0.90 (ddd, *J*=13.0, 10.8, and 5.1 Hz)	0.58 (m)	0.64 (ddd, *J*= 13.0, 10.7 and 5.1 Hz)	1.08 (nd)
15α	1.52 (nd)	1.76 (nd)	1.46 (nd)	1.34 (nd)	2.07 (m)
15β	1.05 (nd)	1.29 (nd)	1.06 (m)	1.18 (nd)	1.66 (nd)
16α	3.78 (16β, s)	2.82 (dd, *J*=10.1, 7.6 Hz)	2.55 (td, *J*= 9.6 and 7.8 Hz)	2.93 (td, *J*= 10.0 and 7.6 Hz)	5.22 (td, *J*= 10.4 and 7.4 Hz)
17α	/	/	3.38 (d, *J*=9.1 Hz)	4.81 (d, *J*=9.8 Hz)	5.43 (d, *J*= 9.9 Hz)
18	0.72 (s)	0.71 (s)	0.65 (s)	0.72 (s)	0.67 (s)
19	0.49 (s)	0.86 (s)	0.86 (s)	0.88 (s)	0.82 (s)
2', 6'	/	2.38 (m) and 2.25 (m)	2.40 (nd) and 2.25 (m)	2.33 (nd)	2.31 (m)
3', 5'	/	1.37 (nd)	1.35 (nd)	1.36 (nd)	1.32 (m)
4'	/	1.21 (nd)	1.21 (nd)	1.21 (nd)	1.17 (m)
17-OCO*C*H$_3$	1.84 (s)	/	/	1.96 (s)	2.00 (s)
3-OCO*C*H$_3$	/	/	/	1.93 (s)	1.96 (s)
17-OH	/	/	4.24 (brs)	/	/
3-OH	/	4.74 (brs)	4.67 (brs)	/	/
2'', 6''	/	2.60 (m) and 2.35 (m)	2.35 (nd)	2.42 (m) and 2.30 (nd)	3.74 (m) and 3.79 (m)
3'', 5''	/	1.36 (m)	1.30 (nd)	1.38 (nd)	1.69 (m), 1.72 (m), and 1.45 (m)
4''	/	1.18 (nd)	1.17 (nd)	1.19 (nd)	
N^+CH_3	/	/	/	/	3.36 (s)

nd = *J*(H,H) were not determined due to the overlapping.

[a] Assignments from ^{1}H–^{1}H COSY, HSQC, and HMBC data in Py-d_5 at 325K.

[b] Coupling constants were obtained by direct inspection of the spectra. Experimental error in the measured ^{1}H–^{1}H coupling constants was ±0.5 Hz.

Table 2
^{13}C NMR data of compounds **8-11**, and **4**.

^{13}C	**8**		**9**		**10**		**11**		**4**	
	$CDCl_3$ [a]	**Py-d_5** [b]	**$CDCl_3$** [a]	**Py-d_5** [b]	**$CDCl_3$** [a]	**Py-d_5** [b]	**$CDCl_3$** [a]	**Py-d_5** [b]	**$CDCl_3$** [c]	**Py-d_5** [b]
1	38.1	38.5	32.6	34.1	32.6	34.4	34.4	34.6	34.2	34.3
2	52.3	51.9	65.1	67.2	65.1	67.2	63.0	63.5	62.9	63.3
3	50.8	50.4	63.4	65.5	63.4	65.6	70.0	69.9	69.7	69.7
4	29.0	29.5	35.0	35.1	35.5	35.5	30.4	30.8	30.2	30.6
5	36.3	36.7	38.4	40.1	38.4	40.0	40.4	40.8	40.1	40.3
6	28.1	28.4	28.2	29.0	28.4	29.4	27.6	28.0	27.3	27.7
7	30.9	31.2	30.7	31.9	31.8	33.1	32.0	32.2	31.5	31.7
8	34.0	34.1	34.4	34.9	34.6	35.4	33.8	34.0	33.5	33.6
9	54.1	54.4	56.5	56.7	56.3	56.8	55.0	55.2	54.4	54.3
10	33.8	34.0	35.9	37.2	35.7	37.1	36.1	36.3	36.0	36.1
11	20.2	20.5	26.7	21.3	21.1	22.0	20.7	21.0	20.6	20.8
12	31.2	31.9	32.2	33.4	38.7	39.9	38.3	38.8	37.6	37.9
13	42.7	43.1	47.7	48.5	43.4	44.6	42.8	42.7	45.1	45.3
14	46.2	46.8	47.0	47.7	48.4	49.5	48.6	48.6	46.3	46.4
15	26.5	26.7	23.1	25.5	27.2	28.3	26.6	26.7	26.9	27.1
16	59.9	59.6	73.0	73.2	65.7	67.0	65.3	65.5	69.9	70.5
17	91.0	91.5	219.2	219.0	77.6	79.6	82.0	82.5	78.6	78.9
18	14.5	14.7	13.7	14.6	13.2	14.2	13.4	13.6	13.3	13.3
19	12.9	12.8	17.5	15.6	17.5	16.1	13.3	13.4	13.1	13.2
2', 6'	/	/	49.5	51.9	49.4	51.8	52.0	52.2	51.9	52.1
3', 5'	/	/	26.1	27.2	26.8	27.6	26.4	27.2	26.3	26.7
4'	/	/	24.8	25.8	24.9	25.9	25.0	25.1	24.7	25.0
17-O*C*OCH$_3$	168.9	168.9	/	/	/	/	170.8	170.2	168.4	169.0
17-OCO*C*H$_3$	21.1	20.8	/	/	/	/	21.3	21.1	21.1	20.9
3-O*C*OCH$_3$	/	/	/	/	/	/	170.4	170.0	170.2	170.0
3-OCO*C*H$_3$	/	/	/	/	/	/	21.5	21.3	21.4	21.3
2'', 6''	/	/	51.4	52.6	53.4	54.4	52.8	53.0	62.0, 60.4	62.1, 60.8
3'', 5''	/	/	20.6	27.5	26.5	27.5	24.6	24.9	20.6, 20.4, and 20.3	20.4, 20.3, and 21.0
4''	/	/	24.2	25.3	24.4	25.5	24.8	25.0		
N$^+$*C*H$_3$	/	/	/	/	/	/	/	/	45.9	45.5

[a] Assignments according to Ref. [12] in $CDCl_3$ at 303K.
[b] Assignments from HSQC and HMBC data in Py-d_5 at 325K.
[c] Assignments according to Ref. [11] in $CDCl_3$ at 325K.

Table 3
^{15}N NMR chemical shifts (ppm)[a] of compounds **9-11**, and **4**.

^{15}N	**9**	**10**	**11**	**4**
1'	48.7	48.5	51.8	51.7
1''	50.0	44.7	45.6	58.6

[a] Assignments from ^{1}H-^{15}N HMBC data in Py-d_5 at 325K using pyridine as the internal reference (pyridine= 317.0 ppm).

In particular, for compound **8** the resonances of all the protons were assigned starting from the characteristic resonances of the epoxy protons H-2β (2.89 ppm), H-3β (2.85 ppm) and H-16β (3.78 ppm), and the proton H-9α (0.36 ppm). For compounds **9-11**, and **4** the ^{1}H NMR chemical shifts of the well recognizable H-2α (2.41, 2.44, 2.26 and 2.23 respectively), H-3β (4.08, 4.06, 5.32, and 5.29 respectively), H-16α (2.82, 2.55, 2.93, and 5.22 respectively), and H-9α (0.58, 0.56, 0.52, and 0.49

respectively) were used as starting point for the interpretation of the ^{1}H NMR spectra, together with H-17α for compounds **10**, **11**, and **4** (3.38, 4.81, and 5.43 respectively).

NOE experiments were performed to confirm the configuration of C-2, C-3, C-16, and C-17 of all the analyzed compounds. In compound **8**, the NOE correlations of H-2 (2.89 ppm) and H-3 (2.85 ppm) with CH_3-19 (0.49 ppm), and of H-16 (3.78 ppm) with CH_3-18 (0.72 ppm) indicated that these protons were on the β face of the ring system, like the group $OCOCH_3$-17, due to the *cis* nature of the epoxide ring. In compounds **9**-**11**, and **4**, the following NOE cross-peaks were observed: H-3/CH_3-19, H-3/H-4β, H-2/H-1α, H–2/H-5α, H-16/H-14α, H-16/H-15α. Finally, for compounds **10**, **11**, and **4**, NOE cross peaks were observed for H-17/H-14α, H-17/H-12α and H-17/H-16α (Figure 3).

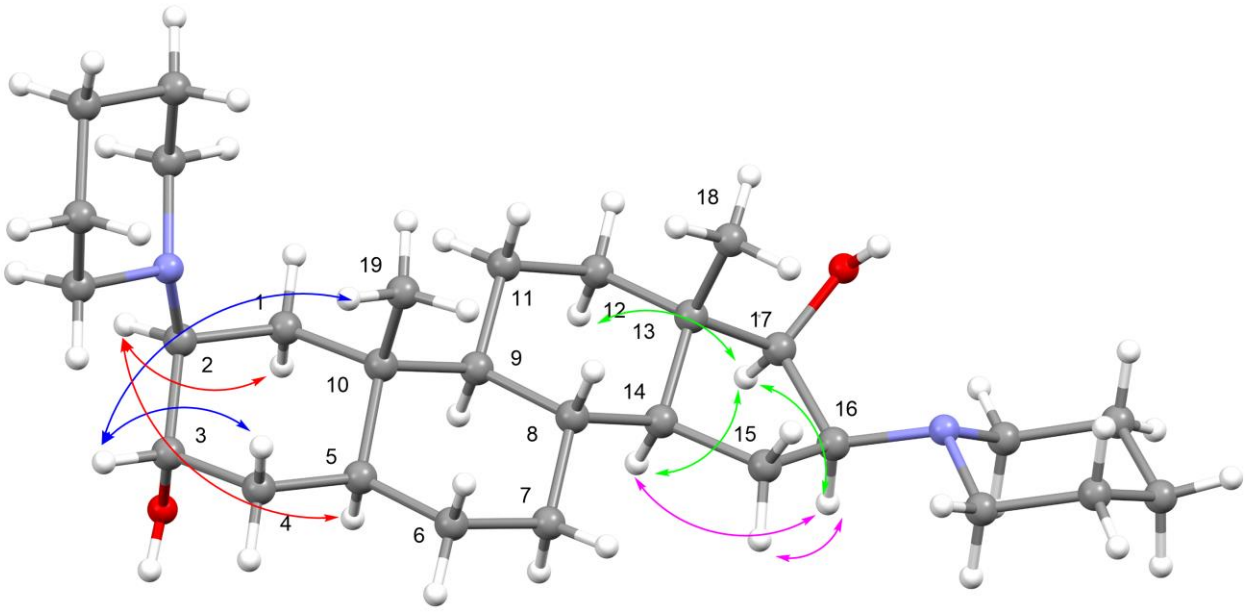

Figure 3. Key NOE correlations of the protons on C-2, C-3, C-16, and C-17 for compound **10**.

In addition, for compounds **9**-**11**, and **4**, the observed $^{3}J_{2\alpha,3\beta}$ (4÷5 Hz) coupling constants suggest that, in pyridine solution, ring A is in chair conformation, while for compounds **10**, **11**, and **4**, the observed $^{3}J_{16\alpha,17\alpha}$ of about 9÷10 Hz indicated an O-C-C-N dihedral angle of about 5° for the D ring, as previously reported for vecuronium bromide (**4**) in $CDCl_3$ [10].

The assignments of carbon atoms of CH, CH_2 and CH_3 groups were confirmed by the gs-HSQC experiment. The quaternary carbon atoms were assigned unambiguously using the information obtained from ^{1}H-^{13}C gs-HMBC experiment. For all the studied compounds, in the ^{1}H-^{13}C gs-HMBC spectra, we observed for C-10 and C-13 the following cross peaks: *H*-2/C-10, C*H*$_3$-19/C-10, *H*-9/C-10, C*H*$_2$-1/C-10, H-4/C-10, and C*H*$_2$-11/C-10; *H*-16/C-13, C*H*$_2$-12/C-13, C*H*$_2$-15/C-13, C*H*$_2$-11/C-13, C*H*$_3$-18/C-13, *H*-14/C-13. For the quaternary C-17 of compound **8**, the following cross peaks

were observed: *H*-16/C-17, OCOC*H*$_3$-17/C-17, C*H*$_2$-15/C-17, and C*H*$_3$-18/C-17. For compound **9** we observed: *H*-16/C-17, C*H*$_2$-15/C-17, C*H*$_2$-12/C-17, *H*-14/C-17, and C*H*$_3$-18/C-17. Following this approach, we found that the ^{13}C resonance assignments of **8-11** and **4** were very close to those reported in the literature for **8-11** [12] and for **4** [11] when analyzed in $CDCl_3$ (see Table 2).

^{1}H-^{15}N HMBC experiments were performed in order to assign the resonances of the two piperidine nitrogens in compounds **9-11** and **4** and to further confirm the hypothesized structure of these compounds. The observed couplings are listed in Table 4.

Table 4
^{1}H-^{15}N gs-HMBC long range couplings observed in the spectra of compounds **9-11**, and **4**.

^{15}N	**HMBC (N→H)**			
	9	**10**	**11**	**4**
1'	H-3β and H-1β	H-3β, C*H*$_2$-1, C*H*$_2$-3', and C*H*$_2$-5'	H-3β, C*H*$_2$-1, C*H*$_2$-3', and C*H*$_2$-5'	H-1α
1''	H-15β	H-17α, H-15β, CH_2-3'', and CH_2-5''	H-17α, H-15β, CH_2-3'', and CH_2-5''	H-17α, N^+C*H*$_3$, and H-15β

[a] Assignments from ^{1}H-^{15}N HMBC data in Py-d_5 at 325K using pyridine as the internal reference (pyridine = 317.0 ppm).

The value of the chemical shift of N-1' changes from 48.7 ppm and 48.5 ppm for compounds **9** and **10** (with free hydroxyl group at the position 3) to 51.8 ppm and 51.7 ppm for **11** and **4**, in which the hydroxyl group at position 3 is acetylated. Moreover, N-1'' is affected by the neighboring substituents; hence, its chemical shift is 50.0, 44.7, or 45.6 depending on the presence of a keto, hydroxyl, or acetoxy group at position 17, respectively. With its quaternarization, N-1'' is deshielded and reaches a value of 58.6 ppm.

3.3 X-Ray and Hirshfeld surface analysis

Compound **10** crystallized in the monoclinic space group $P2_1$; its molecular structure is shown in Figure 4 as an ORTEP diagram [23].

The X-ray diffraction analysis of the key precursor **10** was performed to confirm the installation of the desired stereochemistry at C15 (arbitrary numbering) and verify the correct configuration of the stereocenters involved in the synthetic pathway.

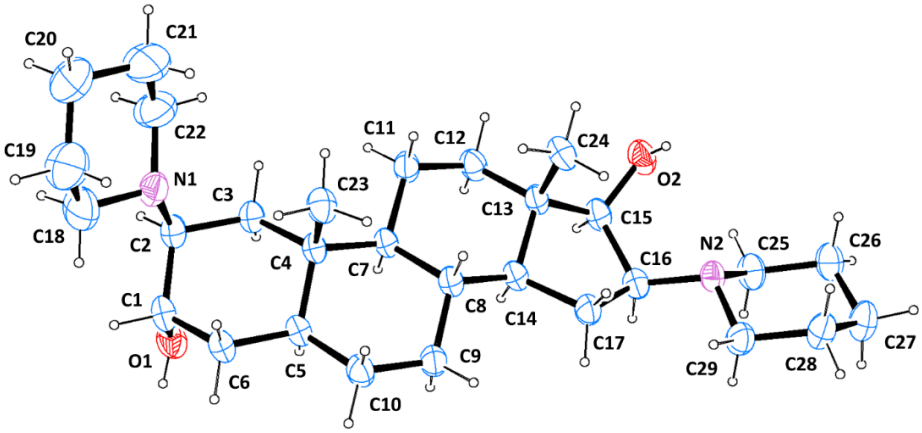

Figure 4. ORTEP diagram of **10**, with the arbitrary atom-numbering scheme.

The crystallographic data allowed the complete stereochemical assignment of the stereogenic carbons: their absolute configuration was defined based on the known enantiomeric arrangement of C4, C5, C7, C8, C13, and C14 (arbitrary numbering), which were unaffected by the synthetic process. Consequently, it was possible to unambiguously establish the stereochemistry of (*S*)-C15 and confirm the configurations of (*S*)-C1, (*S*)-C2, and (*S*)-C16.

The molecular structure of **10** is characterized by a tetracyclic skeleton, formed by three condensed hexatomic rings fused to a cyclopentane, all in *trans* configuration. Rings A, B, and C showed a "chair" conformation; their Cremer-Pople puckering parameters [27] were $\theta = 176.80°$, $\varphi = 150.89°$, $Q_T = 0.5710$ for A, $\theta = 173.59°$, $\varphi = -144.00°$, $Q_T = 0.5764$ for B, and $\theta = 176.16°$, $\varphi = 28.77°$, $Q_T = 0.5702$ for C. The distances of the lower and upper corner carbons from the best mean plane of the remaining ring atoms were as follows: 0.6821 Å (C1) and 0.6644 Å (C4) for ring A, 0.6967 Å (C5) and 0.6313 Å (C8) for ring B, 0.6452 Å (C7) and 0.6991 Å (C13) for ring C. The pentatomic cycle D exhibited a distorted envelope conformation, with C14 at 0.7090 Å from the mean plane identified by C13/C15/C16/C17. Finally, the two piperidine substituents were both in a "chair" conformation: their puckering parameters were $\theta = 177.23°$, $\varphi = -13.59°$, $Q_T = 0.5765$ for the C2-ring, and $\theta = 174.88°$, $\varphi = -173.86°$, $Q_T = 0.5756$ for the C16-ring. The distances of C20 and N1 from the mean plane identified by C18/C19/C21/C22 were 0.6588 Å and 0.6827 Å, respectively. Similarly, the distances of C27 and N2 from the mean plane of the remaining atoms of the ring were 0.6398 Å and 0.7033 Å, respectively.

The crystal packing was ensured by two H-bonds, namely O1-H1X···N2 and O2-H2X···O1, and minor hydrophobic interactions. The HS analysis of **10** revealed that H···H contacts were by far dominant (93.4%); O···H/H···O and N···H/H···N interactions only made up for 5.5% and 1.2% of the intermolecular contacts, respectively. Nevertheless, these strong H-bond interactions were the main

determinants of the stabilization of the crystal packing. A detailed discussion can be found in the Supporting Information.

4. Conclusion

Vecuronium bromide is an amino steroid extensively used in anesthesiology practice as NMBA since 1982. Although its first synthesis dates to 1965, only a few spectroscopic and crystallographic studies are reported in the literature for vecuronium bromide (**4**) and its advanced synthetic intermediates. With the aim of providing new and comprehensive data, we proceeded with the synthesis of these compounds. Starting from the commercially available epiandrosterone (**12**), an optimized synthetic process, avoiding the use of the hazardous bromomethane and improving the yield of the acetylation of intermediate **10** (91% instead of 39% reported for the traditional synthesis), allowed the obtainment of **4** in 7% overall yield (30% yield from **8**). The complete assignment of ^{1}H, ^{13}C, and ^{15}N NMR signals of **4** and its synthetic intermediates was carried out, together with a solid-state analysis of **10**, a key compound having all the stereocenters in the final configuration and suitable for the synthesis of **4**, as well as of pancuronium bromide (**2**) and rapacuronium bromide (**6**). The solid-state investigation was instrumental to substantiate the results of the synthetic and NMR studies in terms of stereochemistry. The HS analysis supported the characterization of the intermolecular contacts, underlying the molecular packing and observed conformation of **4**. Notably, this investigation constitutes the first detailed analysis of a convenient intermediate for the synthesis of multiple NMBAs. The definition of the structural features of the molecule, definitively completing its analytical characterization, may prove invaluable to streamline the drug development and production processes. Furthermore, it may allow to hypothesize relationships between the three-dimensional architecture and the pharmacological properties of this class of compounds.

CRediT authorship contribution statement

Samuele Ciceri: Investigation, Writing - original draft, Writing - review & editing. Diego Colombo: Investigation, Review & editing. Patrizia Ferraboschi: Conceptualization, Review & editing. Paride Grisenti: Conceptualization. Marco Iannone: Investigation. Matteo Mori: Investigation, Writing - review & editing. Fiorella Meneghetti: Investigation, Writing - review & editing.

Declaration of Competing Interest

The authors declare that they have no known competing financial interests or personal relationships that could influence the work reported in this paper.

Acknowledgments

The authors most gratefully thank Prof. Diego G. Gatta for granting access to the instrumentation of the X-ray diffraction platform of the Department of Earth Sciences "Ardito Desio" of the University of Milan. They also wish to acknowledge Dr. Nicola Rotiroti for his kind and helpful support. S.C. acknowledges the financial support (study and research fellowship) provided by Farmhispania S.A. (Barcelona, Spain) in 2020.

Appendix A. Supplementary data

Supplementary data to this article can be found online at http://xxxxx

References

[1] J. Appiah-Ankam, J.M. Hunter, Pharmacology of neuromuscular blocking drugs, BJA Educ. 4(1) (2004) 2-7. https://doi.org/10.1093/bjaceaccp/mkh002.

[2] M.C. McManus, Neuromuscular blockers in surgery and intensive care, Part 1, Am. J. Health Syst. Pharm. 58(23) (2001) 2287-99. https://doi.org/10.1093/ajhp/58.23.2287.

[3] T. Zoltan, M. Sandor, E.S. Vizi, Synthesis and structure-activity relationships of neuromuscular blocking agents, Curr. Med. Chem. 9(16) (2002) 1507-1536. https://doi.org/10.2174/0929867023369466.

[4] F. Donati, Neuromuscular blocking drugs for the new millennium: current practice, future trends--comparative pharmacology of neuromuscular blocking drugs, Anesth. Analg. 90(5 Suppl) (2000) S2-6. https://doi.org/10.1097/00000539-200005001-00002.

[5] C.L. Hewett, D.S. Savage, Improvements in or relating to new 2β,16β-diamino-androstanes, 1965. GB1138605.

[6] Chapter 8 - Relaxation of the skeletal muscles, in: K.W. Clarke, C.M. Trim, L.W. Hall (Eds.), Veterinary Anaesthesia (Eleventh Edition), W.B. Saunders, Oxford, 2014, pp. 169-194.

[7] C.G. Stauble, M. Blobner, The future of neuromuscular blocking agents, Curr. Opin. Anaesthesiol. 33(4) (2020) 490-498. https://doi.org/10.1097/ACO.0000000000000891.

[8] World Health Organization Model List of Essential Medicines, 21st List, 2019. Geneva: World Health Organization. https://www.who.int/publications/i/item/WHOMVPEMPIAU2019.06, 2019 (accessed 05 July 2021).

[9] W.R. Buckett, C.L. Hewett, D.S. Savage, Pancuronium bromide and other steroidal neuromuscular blocking agents containing acetylcholine fragments, J. Med. Chem. 16(10) (1973) 1116-24. https://doi.org/10.1021/jm00268a011.

[10] H. Kooijman, V.J. Van Geerestein, P. Van der Sluis, J.A. Kanters, J. Kroon, C.W. Funke, J. Kelder, Molecular structure of vecuronium bromide, a neuromuscular blocking agent. Crystal structure, molecular mechanics and NMR investigations, J. Chem. Soc., Perkin Trans. 2 (10) (1991) 1581. https://doi.org/10.1039/P29910001581.

[11] L. Fielding, ^{1}H and ^{13}C NMR studies of some steroidal neuromuscular blocking drugs: solution conformations and dynamics, Magn. Reson. Chem. 36(6) (1998) 387-397. https://doi.org/10.1002/(SICI)1097-458X(199806)36:6%3C387::AID-OMR282%3E3.0.CO;2-2.

[12] H. Jiang, N. Jiang, S.-j. Tu, F. Gu, Y.-j. Feng, Structure elucidation of androstane intermediate in the synthesis of vecuronium bromide, Bopuxue Zazhi 25(4) (2008) 531-540.

[13] P. Ferraboschi, M. Chiara Sala, R. Stradi, L. Ragonesi, C. Gagliardi, P. Lanzarotti, E.M. Ragg, M. Mori, F. Meneghetti, Full spectroscopic characterization of two crystal pseudopolymorphic forms of the antiandrogen cortexolone 17α-propionate for topic application, Steroids 128 (2017) 95-104. https://doi.org/10.1016/j.steroids.2017.09.003.

[14] P. Ferraboschi, P. Ciuffreda, S. Ciceri, P. Grisenti, C. Castellano, F. Meneghetti, Crystallographic and spectroscopic study on a known orally active progestin, Steroids 104 (2015) 137-44. https://doi.org/10.1016/j.steroids.2015.09.007.

[15] F. Meneghetti, P. Ferraboschi, P. Grisenti, S. Reza Elahi, M. Mori, S. Ciceri, Crystallographic and NMR investigation of ergometrine and methylergometrine, two alkaloids from *claviceps purpurea*, Molecules 25(2) (2020). https://doi.org/10.3390/molecules25020331.

[16] J. Iriarte, G. Rosenkranz, F. Sondheimer, Steroids. LXV. A synthesis of androsterone, J. Org. Chem. 20 (1955) 542. https://doi.org/10.1021/jo01122a018.

[17] Z. Tuba, Synthesis of 2β,16β-bis-(4'-dimethyl-1'-piperazino)-3α,17β-diacetoxy-5α-androstane dibromide and related compounds, Arzneimittelforschung 30(2a) (1980) 342-6.

[18] Z. Tuba, S. Maho, G. Szabo, G. Galik, G. Balogh, Environmentally-friendly process for the synthesis of quaternary ammonium-steroids, 2006. WO2006038047.
[19] D.N. Kirk, S.J. Gaskell, B.A. Marples, Spectroscopic methods of steroid analysis, Blackie, 1995, p. 25-113. https://doi.org/10.1007/978-94-017-3078-5_2.
[20] H. Fritz, Nitrogen-15 NMR spectroscopy - applications in heterocyclic chemistry, Bull. Soc. Chim. Belg. 93(7) (1984) 559.
[21] M.C. Burla, R. Caliandro, B. Carrozzini, G.L. Cascarano, C. Cuocci, C. Giacovazzo, M. Mallamo, A. Mazzone, G. Polidori, Crystal structure determination and refinement via SIR2014, J. Appl. Crystallogr. 48(1) (2015) 306-309. https://doi.org/10.1107/S1600576715001132.
[22] G. Sheldrick, Crystal structure refinement with SHELXL, Acta Cryst. C 71(1) (2015) 3-8. https://doi.org/10.1107/S2053229614024218.
[23] L. Farrugia, WinGX and ORTEP for Windows: an update, J. Appl. Crystallogr. 45(4) (2012) 849-854. https://doi.org/10.1107/S0021889812029111.
[24] M. Nardelli, PARST95 - an update to PARST: a system of Fortran routines for calculating molecular structure parameters from the results of crystal structure analyses, J. Appl. Crystallogr. 28(5) (1995) 659. https://doi.org/10.1107/S0021889895007138.
[25] C.F. Macrae, I. Sovago, S.J. Cottrell, P.T.A. Galek, P. McCabe, E. Pidcock, M. Platings, G.P. Shields, J.S. Stevens, M. Towler, P.A. Wood, Mercury 4.0: from visualization to analysis, design and prediction, J. Appl. Crystallogr. 53(1) (2020) 226-235. https://doi.org/10.1107/S1600576719014092.
[26] Turner, M.J.; McKinnon, J.J.; Wolff, S.K.; Grimwood, D.J.; Spackman, P.R.; Jayatilaka, D.; Spackman, M.A.; CrystalExplorer17. University of Western Australia. http://crystalexplorer.scb.uwa.edu.au/, 2017 (accessed on 05 July 2021).
[27] D. Cremer, J.A. Pople, Molecular orbital theory of the electronic structure of organic compounds. XXIII. Pseudorotation in saturated five-membered ring compounds, J. Am. Chem. Soc. 97(6) (1975) 1358-1367. https://doi.org/10.1021/ja00839a012.